

# Synthesis of MDM2-p53 Inhibitor BI-0282 via a Dipolar Cycloaddition and Late-Stage Davis–Beirut Reaction

Juergen Ramharter,\* Michael Kulhanek, Maike Dettling, Gerhard Gmaschitz, Jale Karolyi-Oezguer, Harald Weinstabl, and Andreas Gollner\*



Cite This: *Org. Process Res. Dev.* 2022, 26, 2526–2531



Read Online

ACCESS |

Metrics & More

Article Recommendations

Supporting Information

**ABSTRACT:** Herein, we report the structure and synthesis of the potent MDM2-p53 inhibitor BI-0282. The complex spirooxindole scaffold bearing four stereocenters embedded in a rigid polycyclic ring-system was effectively prepared on a multi-gram scale in only five synthesis steps employing a three-component 1,3-dipolar cycloaddition and a late-stage Davis–Beirut reaction as key steps.

**KEYWORDS:** MDM2 inhibitor, cycloaddition, Davis–Beirut reaction, multicomponent reaction, spirooxindole, indazole

## INTRODUCTION

Evasion of apoptosis is a hallmark of cancer and inactivation of the tumor protein p53 (TP53) is a central mechanism of tumor cells to promote their survival and maintain proliferation.<sup>1–3</sup> Based on its central role in preventing the initiation, maintenance, and progression of cancer, TP53 represents one of the most sought-after drug targets in oncology. TP53 is one of the most frequently mutated genes in cancer.<sup>4,5</sup> In TP53 wild-type tumors, the function of TP53 is very often attenuated by mechanisms other than inactivation by mutation or deletion of the TP53 gene, including overexpression of its key negative regulator human MDM2, also known as HDM2, which is the human homologue of mouse double minute 2 (MDM2). MDM2, an E3 ligase, regulates TP53 function and protein stability.<sup>6–8</sup>

A number of structurally distinct, non-peptide, small-molecule inhibitors of the MDM2–TP53 interaction have recently been designed and advanced into clinical studies as a novel approach to cancer therapy for patients with TP53 wild-type tumors.<sup>9–11</sup>

Spirooxindoles have been identified as a privileged structural class to inhibit the MDM2-p53 protein–protein interaction.<sup>12,13</sup> Pioneering work by Wang and co-workers covers the discovery of spiro[3*H*-indole-3,3'-pyrrolidin]-2(1*H*)-ones and its optimization to the clinical candidate MI-77301 (SAR-405838).<sup>14</sup> In a later report, they described the epimerization of this scaffold to four diastereomers in solution by a retro-Mannich/Mannich mechanism which was also shown by X-ray crystallography.<sup>15,16</sup> Two compounds which solved the epimerization problem by the addition of an additional spiro cycle progressed in clinical trials AA-115/APG-115 (Alrizomadlin, Figure 1)<sup>17</sup> and DS-3032 (Milademetan).<sup>18</sup> We identified the spiro[3*H*-indole-3,2'-pyrrolidin]-2(1*H*)-one core as a stable alternative and reported BI-0282 (1), and BI-0252 (2) which showed in vivo efficacy in a SJS-1 xenograft model even when given as a single dose.<sup>19,20</sup> Herein, we report the structure and synthesis of compound 1 which

This work:

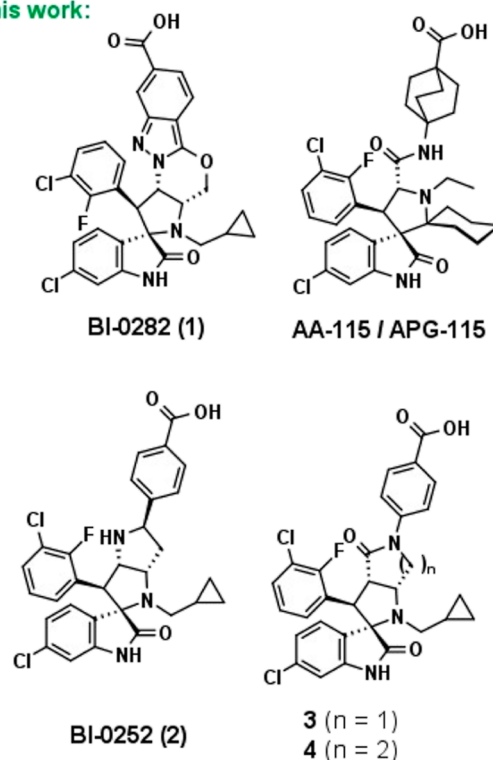
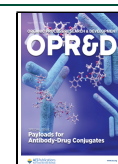


Figure 1. Structures of selected spirooxindole MDM2-p53 inhibitors.

Received: June 14, 2022

Published: July 7, 2022

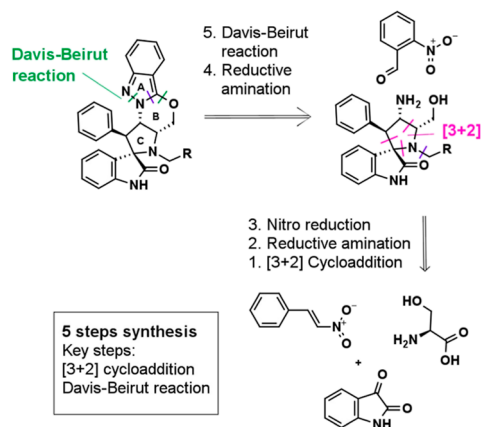


was prepared on a multi-gram scale using a concise five-step synthesis.

## RESULTS AND DISCUSSION

Structurally complex three-dimensional compounds with dense stereochemistry are frequently reported as inhibitors of PPIs and especially for the interaction of the proteins MDM2 and p53.<sup>21</sup> Complex and lengthy syntheses are typically needed to get to such compounds which is undesirable for Medicinal Chemists who typically prepare hundreds to thousands of compounds during a lead optimization program. For designing the new spiro-oxindole series, we capitalized on multi-bond forming transformations to enable rapid generation of structural complexity. We applied a three component [3 + 2] cycloaddition for the synthesis of **2** and reported a novel intramolecular cycloaddition for compounds **3** and **4** (Figure 1).<sup>20,22</sup> Aiming for further potency and improvement of PK properties, we found that the rigidified fused-indazole motive (Scheme 1) had promising properties and optimized this series to obtain **1**.

### Scheme 1. Retrosynthetic Analysis



For the synthesis, we envisioned a sequence including two multi-bond generating steps, a Davis–Beirut reaction to construct the annulated indazole and close rings A and B (Scheme 1), and a [3 + 2] cycloaddition to build up the spirooxindole core structure. This would enable a concise five-step process for the racemic target molecule, followed by a preparative chiral separation of the enantiomers.

Our synthesis (Scheme 2) started with a decarboxylative 1,3-dipolar cycloaddition of commercially available nitrostyrene **5** with *L*-serine and 6-chloroisatin in refluxing MeOH which gave racemic compound **6a** together with regioisomer **6b** as the main products. Especially on large scale effortless separation of isomers greatly ensures the feasibility of a synthetic route. To our delight, precipitation from dichloromethane provided exclusively pure spirooxindole **6a** with acceptable 30% yield. Purification of the mother liquor yielded the regioisomer **6b** in 44% yield and other minor isomers which have not been separated and analyzed. The mechanism of three-component cycloadditions using nitrostyrenes, isatins, and amino acids was the subject of several studies.<sup>23–28</sup> Following the first key step, compound **8** was obtained by the reductive amination of cycloaddition product **6a** with commercial cyclopropylcarboxaldehyde and subsequent nitro group reduction with Raney nickel and H<sub>2</sub> in excellent yield. Amine **8** was reacted with

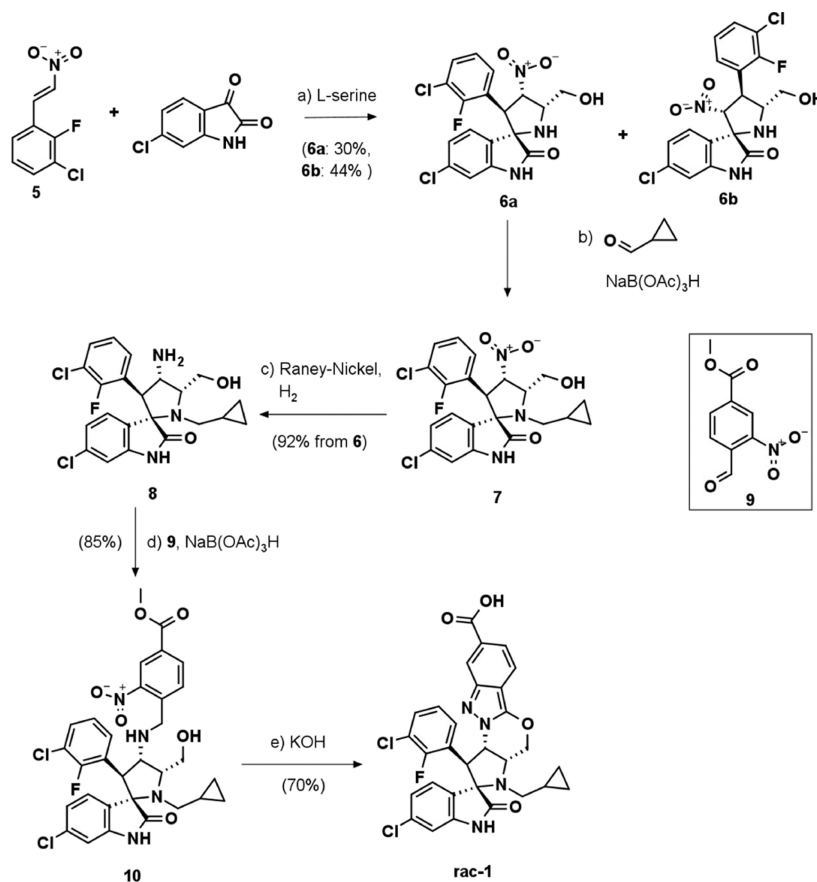
commercial 4-formyl-3-nitrobenzoic acid methyl ester (**9**), in a second reductive amination reaction in acetic acid using sodium triacetoxyborohydride as the reducing agent which gave compound **10** in excellent yields and could be used as the crude product for the next transformation. The final step of the sequence incorporates a Davis–Beirut reaction which initially has been reported by Kurth and Haddadin in 2005.<sup>29,30</sup> Gratifyingly, the intra-molecular annulation reaction and simultaneous saponification of the methyl ester proceeded smoothly at room temperature in very good yields to give racemic **1** which could be readily separated in its enantiomers by chiral SFC. This concise and straight forward five-step sequence enabled the targeted synthesis of a complex molecule with four stereocenters and six-annulated rings in a very efficient and green manner without using complex metal catalysts, ligands, protecting groups, or special reaction conditions (dry solvent, low temperature, argon, or nitrogen atmosphere). Analyzing the sequence according to the definition of an “ideal synthesis” by Gaich and Baran, it achieves a high percentage score of 80%.<sup>31</sup> The sequence was successfully scaled up to >25 g of product per batch without significantly affecting the yield.

## CONCLUSIONS

In summary, we reported the synthesis of MDM2-p53 inhibitor **1** which was selected for further pharmacological studies and preclinical development. Noteworthy, the synthesis was accomplished by the application of two multi-bond forming reactions, a dipolar cycloaddition, and a Davis–Beirut reaction and shows the power of such transformation to access a complex chemical matter in an efficient manner. This concise five-step sequence enabled the synthesis of racemic **1** on a large scale (>25 g).

## EXPERIMENTAL SECTION

**General.** Unless otherwise indicated, all reactions were carried out in standard commercially available glassware using standard synthetic chemistry methods. Commercial starting materials were used without further purification. Solvents used for reactions were of commercial “dry”- or “extra-dry” or “analytical” grade. All other solvents used were reagent grade. Preparative RP-HPLC was carried out on Agilent or Gilson systems using columns from Waters (Sunfire C18 OBD, 5 or 10 μm, 20 × 50 mm, 30 × 50 mm or 50 × 150 mm; X-Bridge C18 OBD, 5 or 10 μm, 20 × 50, 30 × 50, or 50 × 150 mm) or YMC (Triart C18, 5 or 10 μm, 20 × 50 mm, or 30 × 50 mm). Unless otherwise indicated, compounds were eluted with acetonitrile/water gradients using either acidic (0.2% HCOOH or TFA) or basic water [5 mL 2 M NH<sub>4</sub>HCO<sub>3</sub> + 2 mL NH<sub>3</sub> (32%) made up to 1 L with water]. HRMS data were recorded using a Thermo Scientific Orbitrap Elite hybrid ion trap/Orbitrap spectrometer system with an Ultimate 3000 series LPG-3400XRS pump system. Mass calibration was performed using the Pierce LTQ Velos ESI positive ion calibration solution from Thermo Scientific (lot PF200011, product no. 88323). NMR experiments were recorded on Bruker AVANCE 400 and 500 MHz spectrometers at 298 K. Samples were dissolved in 600 μL of DMSO-*d*<sub>6</sub> and TMS was added as an internal standard. 1D <sup>1</sup>H spectra were recorded with 30° excitation pulses and an interpulse delay of 4.2 s with 64k data points and 20 ppm sweep width. 1D <sup>13</sup>C spectra were recorded with broadband composite pulse decoupling (WALTZ16) and

Scheme 2. Synthesis of rac-1<sup>a</sup>

<sup>a</sup>Reagents and conditions: (a) MeOH, reflux, 2 h, **6a** 30%, **6b** 44%; (b) cyclopropyl-carboxaldehyde (2.0 equiv), AcOH (10.0 equiv), 20 min, 25 °C; (CH<sub>3</sub>COO)<sub>3</sub>BHNa (1.1 equiv), 0–25 °C, 16 h; (c) H<sub>2</sub> (8 bar), Raney nickel (0.05 equiv), MeOH, CH<sub>2</sub>Cl<sub>2</sub>, 25 °C, 24 h, 92% over 2 steps; (d) **9** (1.6 equiv), AcOH, 1 h, 25 °C; (CH<sub>3</sub>COO)<sub>3</sub>BHNa (3.1 equiv), 0 °C, 1 h; 25 °C, 16 h, 85%; and (e) KOH (15.5 equiv), *i*-PrOH, H<sub>2</sub>O, 70%.

an interpulse delay of 3.3 s with 64k data points and a sweep width of 240 ppm. Processing and analysis of 1D spectra were performed with Bruker Topspin 3.0 software. No zero filling was performed and spectra were manually integrated after automatic baseline correction.

**Synthesis. Compounds 6a and 6b.** 6-Chloroisatin (10.2 g, 53.97 mmol), 1-Chloro-2-fluoro-3-[(*E*)-2-nitrovinyl]benzene] (10.9 g, 107.9 mmol), and L-serine (5.7 g, 107.9 mmol) are dissolved in methanol (140 mL) and heated to reflux for 16 h using a DrySyn aluminum heating block. After removing the solvent under reduced pressure, the residue is dissolved in dichloromethane. Partial evaporation of dichloromethane leads to the precipitation of a crude solid, which is removed by filtration and further purified by normal phase column chromatography using cyclohexane and ethyl acetate as solvents to yield compound **6a** (6.82 g, 16.00 mmol) in 30% yield as an amorphous beige solid. The filtrate was purified by normal phase column chromatography using cyclohexane and ethyl acetate as solvents to obtain isomer **6b** (10.2 g, 29.93 mmol, 44%) as an amorphous beige solid. Scale-up: 6-chloroisatin (40 g, 220.3 mmol), 1-chloro-2-fluoro-3-[(*E*)-2-nitrovinyl]benzene] (48.9 g, 242.323 mmol, 1.1 equiv), and L-serine (23.2 g, 220.293 mmol) are dissolved in methanol (500 mL) and heated to reflux for 16 h. Work-up and purification as above. **6a**: <sup>1</sup>H NMR (400 MHz, DMSO-*d*<sub>6</sub>): δ 10.34 (s, 1H), 7.60 (d, *J* = 8.11 Hz, 1H), 7.40–7.49 (m, 3H), 7.17 (t, *J* = 7.98 Hz,

1H), 7.11 (dd, *J* = 1.77, 8.11 Hz, 1H), 6.64 (d, *J* = 1.77 Hz, 1H), 6.16 (t, *J* = 9.89 Hz, 1H), 4.95 (t, *J* = 5.32 Hz, 1H), 4.73 (d, *J* = 10.65 Hz, 1H), 4.32–4.44 (m, 1H), 4.06 (d, *J* = 6.59 Hz, 1H), 3.56 (t, *J* = 5.07 Hz, 3H).

<sup>13</sup>C{<sup>1</sup>H} NMR (101 MHz, DMSO-*d*<sub>6</sub>): δ 179.4, 156.1 (d, <sup>1</sup>*J*<sub>C,F</sub> = 249.4 Hz), 143.9, 134.1, 130.8, 128.0, 127.5, 126.7, 125.9 (d, <sup>3</sup>*J*<sub>C,F</sub> = 4.4 Hz), 122.8 (d, <sup>2</sup>*J*<sub>C,F</sub> = 13.2 Hz), 122.2, 120.0 (d, <sup>2</sup>*J*<sub>C,F</sub> = 19.1 Hz), 109.9, 87.5, 70.9, 62.3, 58.7, 48.3.

HRMS (ESI) *m/z*: [M + H]<sup>+</sup> calcd for C<sub>18</sub>H<sub>15</sub>Cl<sub>2</sub>FN<sub>3</sub>O<sub>4</sub>, 426.0418; found, 426.0429.

**6b**: <sup>1</sup>H NMR (500 MHz, DMSO-*d*<sub>6</sub>): δ 7.59–7.50 (m, 2H), 7.30–7.24 (m, 2H), 7.08 (dd, *J* = 1.9, 7.9 Hz, 1H), 6.87 (d, *J* = 1.9 Hz, 1H), 5.62 (d, *J* = 10.1 Hz, 1H), 4.87 (t, *J* = 5.5 Hz, 1H), 4.43 (t, *J* = 9.8 Hz, 1H), 3.85–3.74 (m, 2H), 3.53–3.45 (m, 1H).

<sup>13</sup>C{<sup>1</sup>H} NMR (126 MHz, DMSO-*d*<sub>6</sub>): δ 179.24, 156.37 (d, <sup>1</sup>*J*<sub>C,F</sub> = 248.0 Hz), 144.42, 135.04, 130.31, 129.29 (d, <sup>3</sup>*J*<sub>C,F</sub> = 3.6 Hz), 126.95, 126.37, 126.28 (d, <sup>2</sup>*J*<sub>C,F</sub> = 12.7 Hz), 126.24 (d, <sup>3</sup>*J*<sub>C,F</sub> = 4.5 Hz), 122.31, 120.47 (d, <sup>2</sup>*J*<sub>C,F</sub> = 18.2 Hz), 110.44, 96.17, 69.18, 64.08, 61.31, 44.37.

HRMS (ESI) *m/z*: [M + H]<sup>+</sup> calcd for C<sub>18</sub>H<sub>14</sub>Cl<sub>2</sub>FN<sub>3</sub>O<sub>4</sub>, 426.0418; found, 426.0429.

**Compound 7.** Compound **6a** (19 g, 44.6 mmol) is dissolved in acidic acid (51 mL, 891.5 mmol) and treated with cyclopropanecarboxaldehyde (6.65 mL, 89.2 mmol). After 20 min, the resulting mixture is cooled with an ice/water bath and sodium triacetoxyborohydride (21.9 g, 95% purity, 98.1 mmol)

is slowly added. The cooling bath is removed, and the mixture is stirred for 16 h. The reaction mixture is carefully quenched with water and diluted dichloromethane. The aqueous layer is extracted with dichloromethane and the organic layers are combined. The solvents are removed under reduced pressure and the residue is dissolved in diethyl ether and washed with saturated sodium hydrogen carbonate solution. The organic layer is dried with sodium sulfate and the solvent evaporated to yield 21.6 g of crude product **7**, which is used without further purification in the next step.

$^1\text{H}$  NMR (400 MHz, DMSO- $d_6$ ):  $\delta$  10.44 (br s, 1H), 7.65 (d,  $J$  = 7.86 Hz, 1H), 7.40–7.46 (m, 1H), 7.37 (t,  $J$  = 7.10 Hz, 1H), 7.06–7.19 (m, 2H), 6.61 (d,  $J$  = 1.77 Hz, 1H), 6.28 (dd,  $J$  = 9.89, 11.66 Hz, 1H), 4.94 (t,  $J$  = 5.58 Hz, 1H), 4.78 (d,  $J$  = 11.66 Hz, 1H), 3.90–3.98 (m, 1H), 3.75–3.86 (m, 1H), 3.66–3.74 (m, 1H), 2.17–2.30 (m, 2H), 0.47–0.64 (m, 1H), 0.26–0.36 (m, 1H), 0.13–0.23 (m, 1H), –0.03 to 0.05 (m, 1H), –0.25 to 0.15 (m, 1H).

$^{13}\text{C}\{^1\text{H}\}$  NMR (101 MHz, DMSO- $d_6$ ):  $\delta$  177.8, 156.2 (d,  $^1J_{\text{C,F}}$  = 248.7 Hz), 143.8, 134.2, 130.8, 127.7, 127.1, 126.6, 125.8 (d,  $^3J_{\text{C,F}}$  = 5.1 Hz), 122.6, 122.3 (d,  $^2J_{\text{C,F}}$  = 13.2 Hz), 120.1 (d,  $^2J_{\text{C,F}}$  = 19.1 Hz), 110.1, 83.7, 74.9, 63.8, 61.3, 55.1, 46.7, 11.3, 5.4, 4.4.

HRMS (ESI)  $m/z$ :  $[\text{M} + \text{H}]^+$  calcd for  $\text{C}_{22}\text{H}_{21}\text{Cl}_2\text{FN}_3\text{O}_4$ , 480.0888; found, 480.0874.

**Compound 8.** Crude intermediate **7** (21.6 g) is dissolved in methanol (192 mL) and dichloromethane (128 mL) and treated with a catalytic amount of Raney nickel (slurry in water). The reaction vessel is pressurized with dihydrogen (8 bar) and the reaction mixture stirred for 24 h. Solids are removed by filtration and the solvent of the filtrate removed under reduced pressure. The residue is redissolved in ethyl acetate and water and treated with diluted aqueous HCl. After extraction of the aqueous layer with ethyl acetate, the combined organic layers are dried with sodium sulfate and the solvent evaporated to yield crude intermediate **8** (20.8 g, 90% purity, 41.6 mmol) in 92% yield over two steps, which is used without further purification in the next step.

$^1\text{H}$  NMR (500 MHz, DMSO- $d_6$ ):  $\delta$  10.30 (br s, 1H), 7.54 (d,  $J$  = 7.9 Hz, 1H), 7.40–7.46 (m, 1H), 7.35 (t,  $J$  = 6.6 Hz, 1H), 7.17–7.23 (m, 1H), 7.11 (dd,  $J$  = 7.9, 1.9 Hz, 1H), 6.60 (d,  $J$  = 1.6 Hz, 1H), 5.24–5.68 (m, 2H), 4.66 (dd,  $J$  = 11.2, 9.3 Hz, 1H), 4.06 (d,  $J$  = 11.7 Hz, 1H), 3.86–3.93 (m, 1H), 3.79–3.84 (m, 1H), 3.46 (dt,  $J$  = 5.8, 2.8 Hz, 1H), 2.26 (qd,  $J$  = 13.3, 6.5 Hz, 2H), 0.52–0.68 (m, 1H), 0.29–0.37 (m, 1H), 0.14–0.24 (m, 1H), 0.00 (m, 1H), –0.17 ppm (m, 1H).

$^{13}\text{C}\{^1\text{H}\}$  NMR (101 MHz, DMSO- $d_6$ ):  $\delta$  178.6, 157.1 (d,  $^1J_{\text{C,F}}$  = 245.8 Hz), 143.7, 133.1, 129.6, 129.2, 128.4, 126.5, 125.4 (d,  $^3J_{\text{C,F}}$  = 4.4 Hz), 125.1 (d,  $^2J_{\text{C,F}}$  = 13.9 Hz), 122.0, 119.6 (d,  $^2J_{\text{C,F}}$  = 19.1 Hz), 109.4, 75.3, 65.1, 62.4, 55.6, 53.8, 52.5, 11.8, 5.5, 4.3.

HRMS (ESI)  $m/z$ :  $[\text{M} + \text{H}]^+$  calcd for  $\text{C}_{22}\text{H}_{23}\text{Cl}_2\text{FN}_3\text{O}_2$ , 450.1146; found, 450.1149.

**Compound 10.** Crude intermediate **8** (20.8 g, 90% purity, 38.8 mmol) is dissolved in acetic acid (59.5 mL) and treated with 4-formyl-3-nitrobenzoic acid methyl ester (13.5 g, 62.4 mmol, **9**). After 1 h, the resulting mixture is cooled with a water bath and sodium triacetoxyborohydride (26.9 g, 120.6 mmol) is slowly added in portions. The cooling bath is removed, and the mixture is stirred for 16 h. The reaction mixture is carefully quenched with water and diluted dichloromethane. The aqueous layer is extracted with dichloromethane and the organic layers are combined. The

solvents are removed under reduced pressure and the residue is dissolved in diethyl ether and washed with saturated sodium hydrogen carbonate solution. The organic layer is dried with sodium sulfate and the solvent evaporated to yield crude intermediate **10** (32.4 g, 70% purity, 35.3 mmol) in 85% yield, which is used directly in the next step.

Scale-up: intermediate **8** (30.0 g, 98.3% purity, 65.485 mmol), 112 mL of acetic acid, 4-formyl-3-nitrobenzoic acid methyl ester (16.944 g, 78.582 mmol, **9**). Using the procedure and work-up as described above gave intermediate **10** (46.46 g, purity 75%, 54.353 mmol) in 83% yield.

$^1\text{H}$  NMR (400 MHz, DMSO- $d_6$ ):  $\delta$  10.18 (s, 1H), 8.26 (d,  $J$  = 1.52 Hz, 1H), 8.12 (dd,  $J$  = 1.52, 8.11 Hz, 1H), 7.69 (d,  $J$  = 8.11 Hz, 1H), 7.56 (d,  $J$  = 7.86 Hz, 1H), 7.32–7.39 (m, 1H), 7.02–7.13 (m, 2H), 6.94–7.01 (m, 1H), 6.55 (d,  $J$  = 1.77 Hz, 1H), 4.85 (br t,  $J$  = 5.58 Hz, 1H), 4.26–4.41 (m, 1H), 4.17 (dd,  $J$  = 6.59, 15.72 Hz, 1H), 3.86–3.99 (m, 7H), 3.69–3.79 (m,  $J$  = 7.00, 9.50 Hz, 1H), 2.68–2.77 (m, 1H), 2.17–2.32 (m, 2H), 0.54–0.67 (m, 1H), 0.27–0.38 (m, 1H), 0.13–0.24 (m, 1H), –0.04 to 0.05 (m, 1H), –0.24 to 0.14 (m, 1H).

$^{13}\text{C}\{^1\text{H}\}$  NMR (101 MHz, DMSO- $d_6$ ):  $\delta$  178.6, 165.0, 156.6 (d,  $^1J_{\text{C,F}}$  = 247.2 Hz), 149.0, 143.6, 141.9, 133.3, 133.2, 131.5, 129.7, 129.6, 129.0, 128.0, 126.6, 125.3, 125.2 (d,  $^2J_{\text{C,F}}$  = 13.2 Hz), 125.0, 122.0, 119.6 (d,  $^2J_{\text{C,F}}$  = 19.1 Hz), 109.5, 74.9, 64.0, 61.9, 59.9, 55.6, 53.2, 51.0, 49.2, 11.7, 5.4, 4.4.

HRMS (ESI)  $m/z$ :  $[\text{M} + \text{H}]^+$  calcd for  $\text{C}_{31}\text{H}_{30}\text{Cl}_2\text{FN}_4\text{O}_6$ , 643.1521; found, 643.1523.

**Compound 1.** Intermediate **10** (28.8 g, 44.8 mmol) is dissolved in isopropanol (300 mL) and a solution of potassium hydroxide (39.0 g, 694.9 mmol) in water (95 mL) is slowly added. After stirring for 16 h at ambient temperature, the solvents are partially removed under reduced pressure. The residue is diluted with ethyl acetate and treated with a diluted aqueous solution of citric acid. After extraction of the aqueous layer with ethyl acetate, the organic layers are combined, dried with sodium sulfate, and the solvent is removed under reduced pressure. Purification by normal phase column chromatography using dichloromethane and methanol as solvents yields **rac-1** (25.8 g, 43.5 mmol) in 70% yield as an amorphous white solid.

Chiral SFC and subsequent purification by reversed phase column chromatography using acetonitrile and methanol as solvents furnishes **1** (BI-0282).

**Rac-1** (60 g, 93.3 mmol) was separated by chiral SFC and reversed phase column chromatography to obtain **1** (24.4 g, 40.0 mmol, 43%) as an amorphous white solid.

Chiral HPLC (CHIRALPAK, heptane/isopropanol/trifluoroacetic acid = 70/30/0.1, flow rate 1.0 mL/min,  $I$  = 240 mM)  $t_R$  = 7.8 min (**1**), and 11.1 min (**ent-1**). Preparative SFC (CHIRALPAK, carbon dioxide/isopropanol + 1% diethylamine) = 70/30, flow rate 300 g/min,  $I$  = 290 nM).

$^1\text{H}$  NMR (500 MHz, DMSO- $d_6$ ):  $\delta$  12.64 (br s, 1H), 10.29 (s, 1H), 7.67 (s, 1H), 7.47 (d,  $J$  = 8.83 Hz, 2H), 7.29–7.36 (m, 1H), 7.26 (d,  $J$  = 7.88 Hz, 1H), 7.21 (dd,  $J$  = 1.26, 8.83 Hz, 1H), 7.12 (t,  $J$  = 8.04 Hz, 1H), 6.92 (dd,  $J$  = 1.89, 7.88 Hz, 1H), 6.48 (d,  $J$  = 1.89 Hz, 1H), 5.86 (t,  $J$  = 9.14 Hz, 1H), 4.59–4.68 (m, 1H), 4.52 (dd,  $J$  = 7.88, 11.35 Hz, 1H), 4.23–4.32 (m, 1H), 4.20 (d,  $J$  = 10.09 Hz, 1H), 2.27 (dd,  $J$  = 7.57, 13.08 Hz, 1H), 2.13 (dd,  $J$  = 5.83, 13.08 Hz, 1H), 0.47–0.62 (m, 1H), 0.26–0.37 (m, 1H), 0.11–0.20 (m, 1H), –0.04 to 0.04 (m, 1H), –0.25 (s, 1H).

$^{13}\text{C}\{^1\text{H}\}$  NMR (125 MHz, DMSO- $d_6$ ):  $\delta$  177.5, 168.1, 156.1 (d,  $^1J_{\text{C,F}}$  = 248.7 Hz), 146.3, 145.3, 144.0, 134.1, 130.3, 129.7,



129.5, 126.8, 126.7, 125.4 (d,  $^3J_{C,F} = 4.4$  Hz), 123.5 (d,  $^2J_{C,F} = 13.2$  Hz), 122.5, 120.0, 119.9, 119.7 (d,  $^2J_{C,F} = 18.3$  Hz), 118.7, 110.0, 107.3, 76.4, 69.2, 57.5, 56.8, 54.2, 51.2, 11.6, 5.5, 4.1.

HRMS (ESI)  $m/z$ :  $[M + H]^+$  calcd for  $C_{30}H_{24}Cl_2FN_4O_4$ , 593.1153; found, 593.1165.

## ■ ASSOCIATED CONTENT

### SI Supporting Information

The Supporting Information is available free of charge at <https://pubs.acs.org/doi/10.1021/acs.oprd.2c00192>.

Experimental procedures, characterization data, and copies of NMR spectra for all products (PDF)

## ■ AUTHOR INFORMATION

### Corresponding Authors

Juergen Ramharter – Boehringer Ingelheim RCV GmbH & Co KG, A-1121 Vienna, Austria; [orcid.org/0000-0001-7618-1862](https://orcid.org/0000-0001-7618-1862); Email: [juergen.ramharter@boehringer-ingelheim.com](mailto:juergen.ramharter@boehringer-ingelheim.com)

Andreas Gollner – Boehringer Ingelheim RCV GmbH & Co KG, A-1121 Vienna, Austria; [orcid.org/0000-0002-4347-8296](https://orcid.org/0000-0002-4347-8296); Email: [andreas.gollner@boehringer-ingelheim.com](mailto:andreas.gollner@boehringer-ingelheim.com)

### Authors

Michael Kulhanek – Boehringer Ingelheim RCV GmbH & Co KG, A-1121 Vienna, Austria

Maike Dettling – Boehringer Ingelheim RCV GmbH & Co KG, A-1121 Vienna, Austria

Gerhard Gmaschitz – Boehringer Ingelheim RCV GmbH & Co KG, A-1121 Vienna, Austria

Jale Karolyi-Oezguer – Boehringer Ingelheim RCV GmbH & Co KG, A-1121 Vienna, Austria

Harald Weinstabl – Boehringer Ingelheim RCV GmbH & Co KG, A-1121 Vienna, Austria; [orcid.org/0000-0003-1308-2730](https://orcid.org/0000-0003-1308-2730)

Complete contact information is available at:

<https://pubs.acs.org/doi/10.1021/acs.oprd.2c00192>

### Author Contributions

The manuscript was written through contributions of all authors. All authors have given approval to the final version of the manuscript.

### Funding

Austrian Research Promotion Agency FFG (grants: 832260, 837815, and 842856).

### Notes

The authors declare the following competing financial interest(s): All authors were full Boehringer Ingelheim RCV GmbH & Co KG full-time employees at the time when this study was performed.

## ■ ACKNOWLEDGMENTS

Boehringer Ingelheim RCV GmbH & Co KG is grateful for financial support by the Austrian Research Promotion Agency FFG. We thank Helmut Berger, David Covini, Geraldine Garavel, Peter Etmayer, Elisabeth Grondal, Wolfgang Hela, Karin Stefanie Hofbauer, Christiane Kofink, Roland Kousek, Norbert Kraut, Moriz Mayer, Darryl B. McConnell, Jörg Rinnenthal, Dorothea Rudolph, Steffen Steurer, Michaela Streicher, Steffen Weik, Patrick Werni, and Tobias Wunberg.

## ■ ABBREVIATIONS

PK, pharmacokinetics; PPI, protein–protein interaction; MDM2, mouse double minute 2; SFC, supercritical fluid company

## ■ REFERENCES

- (1) Lane, D. P. P53, Guardian of the Genome. *Nature* **1992**, *358*, 15–16.
- (2) Hanahan, D. Hallmarks of Cancer: New Dimensions. *Cancer Discov.* **2022**, *12*, 31–46.
- (3) Levine, A. J. p53: 800 million years of evolution and 40 years of discovery. *Nat. Rev. Cancer* **2020**, *20*, 471–480.
- (4) Kandath, C.; McLellan, M. D.; Vandin, F.; Ye, K.; Niu, B.; Lu, C.; Xie, M.; Zhang, Q.; McMichael, J. F.; Wyczalkowski, M. A.; Leiserson, M. D. M.; Miller, C. A.; Welch, J. S.; Walter, M. J.; Wendl, M. C.; Ley, T. J.; Wilson, R. K.; Raphael, B. J.; Ding, L. Mutational landscape and significance across 12 major cancer types. *Nature* **2013**, *502*, 333–339.
- (5) Lawrence, M. S.; Stojanov, P.; Mermel, C. H.; Robinson, J. T.; Garraway, L. A.; Golub, T. R.; Meyerson, M.; Gabriel, S. B.; Lander, E. S.; Getz, G. Discovery and saturation analysis of cancer genes across 21 tumour types. *Nature* **2014**, *505*, 495–501.
- (6) Momand, J.; Zambetti, G. P.; Olson, D. C.; George, D.; Levine, A. J. The MDM2 oncogene product forms a complex with the p53 protein and inhibits p53-mediated transactivation. *Cell* **1992**, *69*, 1237–1245.
- (7) Tao, W.; Levine, A. J. Nucleocytoplasmic shuttling of oncoprotein HDM2 is required for HDM2-mediated degradation of p53. *Proc. Natl. Acad. Sci. U.S.A.* **1999**, *96*, 3077–3080.
- (8) Haupt, Y.; Maya, R.; Kazaz, A.; Oren, M. MDM2 promotes the rapid degradation of p53. *Nature* **1997**, *387*, 296–299.
- (9) Konopleva, M.; Martinelli, G.; Daver, N.; Papayannidis, C.; Wei, A.; Higgins, B.; Ott, M.; Mascarenhas, J.; Andreeff, M. MDM2 Inhibition: An Important Step Forward in Cancer Therapy. *Leukemia* **2020**, *34*, 2858–2874.
- (10) Wang, S.; Zhao, Y.; Aguilar, A.; Bernard, D.; Yang, C.-Y. Targeting the MDM2–P53 Protein–Protein Interaction for New Cancer Therapy: Progress and Challenges. *Cold Spring Harbor Perspect. Med.* **2017**, *7*, a026245.
- (11) Zak, K.; Pecak, A.; Rys, B.; Wladyka, B.; Dömling, A.; Weber, L.; Holak, T. A.; Dubin, G. Mdm2 and MdmX inhibitors for the treatment of cancer: a patent review (2011–present). *Expert Opin. Ther. Pat.* **2013**, *23*, 425–448.
- (12) Gupta, A. K.; Bharadwaj, M.; Kumar, A.; Mehrotra, R. Spiro-Oxindoles as a Promising Class of Small Molecule Inhibitors of P53–MDM2 Interaction Useful in Targeted Cancer Therapy. *Top. Curr. Chem.* **2017**, *375*, 3.
- (13) Ding, K.; Lu, Y.; Nikolovska-Coleska, Z.; Qiu, S.; Ding, Y.; Gao, W.; Stuckey, J.; Krajewski, K.; Roller, P. P.; Tomita, Y.; Parrish, D. A.; Deschamps, J. R.; Wang, S. Structure-Based Design of Potent Non-Peptide MDM2 Inhibitors. *J. Am. Chem. Soc.* **2005**, *127*, 10130–10131.
- (14) Wang, S.; Sun, W.; Zhao, Y.; McEachern, D.; Meaux, I.; Barrière, C.; Stuckey, J. A.; Meagher, J. L.; Bai, L.; Liu, L.; Hoffman-Luca, C. G.; Lu, J.; Shangary, S.; Yu, S.; Bernard, D.; Aguilar, A.; Dos-Santos, O.; Besret, L.; Guerif, S.; Pannier, P.; Gorge-Bernat, D.; Debussche, L. SAR405838: An Optimized Inhibitor of MDM2–P53 Interaction That Induces Complete and Durable Tumor Regression. *Cancer Res.* **2014**, *74*, 5855–5865.
- (15) Zhao, Y.; Liu, L.; Sun, W.; Lu, J.; McEachern, D.; Li, X.; Yu, S.; Bernard, D.; Ochsenbein, P.; Ferey, V.; Carry, J.-C.; Deschamps, J. R.; Sun, D.; Wang, S. Diastereomeric Spirooxindoles as Highly Potent and Efficacious MDM2 Inhibitors. *J. Am. Chem. Soc.* **2013**, *135*, 7223–7234.
- (16) Popowicz, G. M.; Czarna, A.; Wolf, S.; Wang, K.; Wang, W.; Dömling, A.; Holak, T. A. Structures of Low Molecular Weight Inhibitors Bound to MDMX and MDM2 Reveal New Approaches for

P53-MDMX/MDM2 Antagonist Drug Discovery. *Cell Cycle* **2010**, *9*, 1104–1111.

(17) Aguilar, A.; Lu, J.; Liu, L.; Du, D.; Bernard, D.; McEachern, D.; Przybranowski, S.; Li, X.; Luo, R.; Wen, B.; Sun, D.; Wang, H.; Wen, J.; Wang, G.; Zhai, Y.; Guo, M.; Yang, D.; Wang, S. Discovery of 4-((3'R,4'S,S'R)-6'-Chloro-4'-(3-chloro-2-fluorophenyl)-1'-ethyl-2'-oxodispiro[cyclohexane-1,2'-pyrrolidine-3',3''-indoline]-5'-carboxamido)bicyclo[2.2.2]octane-1-carboxylic Acid (AA-115/APG-115): A Potent and Orally Active Murine Double Minute 2 (MDM2) Inhibitor in Clinical Development. *J. Med. Chem.* **2017**, *60*, 2819–2839.

(18) Takahashi, S.; Fujiwara, Y.; Nakano, K.; Shimizu, T.; Tomomatsu, J.; Koyama, T.; Ogura, M.; Tachibana, M.; Kakurai, Y.; Yamashita, T.; Sakajiri, S.; Yamamoto, N. Safety and Pharmacokinetics of Milademetan, a MDM2 Inhibitor, in Japanese Patients with Solid Tumors: A Phase I Study. *Cancer Sci.* **2021**, *112*, 2361–2370.

(19) Ramharter, J.; Broeker, J.; Gille, A.; Gollner, A.; Henry, M.; Toelle, N.; Weinstabl, H. Preparation of new spiro[3H-indole-3,2'-pyrrolidin]-2(1H)-one compounds and derivatives as MDM2-p53 inhibitors. Patent WO 2016026937 A1, 2016.

(20) Gollner, A.; Rudolph, D.; Arnhof, H.; Bauer, M.; Blake, S. M.; Boehmelt, G.; Cockroft, X.-L.; Dahmann, G.; Ettmayer, P.; Gerstberger, T.; Karolyi-Oezguer, J.; Kessler, D.; Kofink, C.; Ramharter, J.; Rinnenthal, J.; Savchenko, A.; Schnitzer, R.; Weinstabl, H.; Weyer-Czernilofsky, U.; Wunberg, T.; McConnell, D. B. Discovery of Novel Spiro[3H-Indole-3,2'-Pyrrolidin]-2(1H)-One Compounds as Chemically Stable and Orally Active Inhibitors of the MDM2–P53 Interaction. *J. Med. Chem.* **2016**, *59*, 10147–10162.

(21) Ran, X.; Gestwicki, J. E. Inhibitors of Protein-Protein Interactions (PPIs): An Analysis of Scaffold Choices and Buried Surface Area. *Curr. Opin. Chem. Biol.* **2018**, *44*, 75–86.

(22) Gollner, A.; Weinstabl, H.; Fuchs, J. E.; Rudolph, D.; Garavel, G.; Hofbauer, K. S.; Karolyi-Oezguer, J.; Gmaschitz, G.; Hela, W.; Kerres, N.; Grondal, E.; Werni, P.; Ramharter, J.; Broeker, J.; McConnell, D. B. Targeted Synthesis of Complex Spiro[3H-indole-3,2'-pyrrolidin]-2(1H)-ones by Intramolecular Cyclization of Azomethine Ylides: Highly Potent MDM2–p53 Inhibitors. *ChemMedChem* **2019**, *14*, 88–93.

(23) Chen, G.; Yang, J.; Gao, S.; Zhang, Y.; Hao, X. Theoretical study of regioselectivity in the synthesis of spiro [pyrrolidine-2,3'-oxindole] compounds by [3 + 2] cycloaddition. *Res. Chem. Intermed.* **2015**, *41*, 4987–4996.

(24) Alimohammadi, K.; Sarrafi, Y.; Tajbakhsh, M.; Yeganegi, S.; Hamzehloueian, M. An experimental and theoretical investigation of the regio- and stereoselectivity of the polar [3 + 2] cycloaddition of azomethine ylides to nitrostyrenes. *Tetrahedron* **2011**, *67*, 1589–1597.

(25) Rajesh, S. M.; Perumal, S.; Menéndez, J. C.; Yogeewari, P.; Sriram, D. Antimycobacterial activity of spirooxindolo-pyrrolidine, pyrrolizine and pyrrolothiazole hybrids obtained by a three-component regio- and stereoselective 1,3-dipolar cycloaddition. *MedChemComm* **2011**, *2*, 626–630.

(26) Poornachandran, M.; Raghunathan, R. Synthesis of spirooxindolo/spiroindano nitro pyrrolizidines through regioselective azomethine ylide cycloaddition reaction. *Synth. Commun.* **2007**, *37*, 2507–2517.

(27) Izmet'ev, A. N.; Gazieva, G. A.; KravchenkoChen, G. Regioselectivity of (3+2) cycloaddition of azomethine ylides to activated olefins in the synthesis of spiro[oxindole-3,2'-pyrrolidine] derivatives. *Chem. Heterocycl. Compd.* **2020**, *56*, 255.

(28) Chen, G.; Yang, J.; Gao, S.; He, H.; Li, S.; Di, Y.; Chang, Y.; Lu, Y.; Hao, X. Spiro[pyrrolidine-2,3'-oxindole] derivatives synthesized by novel regioselective 1,3-dipolar cycloadditions. *Mol. Diversity* **2012**, *16*, 151–156.

(29) Kurth, M. J.; Olmstead, M. M.; Haddadin, M. J. Claimed 2,1-Benzisoxazoles Are Indazalones. *J. Org. Chem.* **2005**, *70*, 1060–1062.

(30) Zhu, J. S.; Haddadin, M. J.; Kurth, M. J. Davis–Beirut Reaction: Diverse Chemistries of Highly Reactive Nitroso Inter-

mediates in Heterocycle Synthesis. *Acc. Chem. Res.* **2019**, *52*, 2256–2265.

(31) Gaich, T.; Baran, P. S. Aiming for the Ideal Synthesis. *J. Org. Chem.* **2010**, *75*, 4657–4673.